Supplementary information

Mesopore-stimulated electromagnetic near-field: electrochemical synthesis of mesoporous copper films by micelle self-assembly

Hyunsoo Lim,[a] Dabum Kim,[b] Yena Kim,[c] Tomota Nagaura,[a] Jungmok You,[b] Jeonghun Kim,[d] Hyun-Jong Kim,[e] Jongbeom Na,[a,*] Joel Henzie,[c,*] and Yusuke Yamauchi[a,b,c,*]

[a] *Australian Institute for Bioengineering and Nanotechnology (AIBN) and School of Chemical Engineering, The University of Queensland, Brisbane, QLD, 4072, Australia.*

[b] *Department of Plant & Environmental New Resources, Kyung Hee University, 1732 Deogyeong-daero, Giheung-gu, Yongin-si, Gyeonggi-do 446-701, South Korea.*

[c] *International Center for Materials Nanoarchitechtonics (MANA), National Institute for Materials Science (NIMS), 1-1 Namiki, Tsukuba, Ibaraki 305-0044, Japan.*

[d] *Department of Chemistry, Kookmin University, 77 Jeongneung-ro, Seongbuk-gu, Seoul, 02707, Republic of Korea.*

[e] *Surface Technology Group, Korea Institute of Industrial Technology (KITECH), Incheon, 21999, Republic of Korea*

Supplementary note 1

1. The estimation of the molecular number for a reference

   10^{-1} M of R6G aqueous solution was fabricated. For the accurate molecular numbers excited by a laser, a 20x objective lens (LEICA) with 1.1 mm of the beam waist and a cylindrical container with 1.6 mm depth were used. This gives us the accurate number of excited molecules by the 785 nm laser beam by following the equation:

   $$V = \frac{1}{2} \cdot D \cdot \pi \cdot h$$

   where D is the beam waist and h is the height of the cylinder. By multiplying the concentration of the solution (in molecules/micron2) to the beam volume, we can estimate the number of molecules excited in the Raman reference measurement (NRef).

2. The estimation of the molecular number on MCuFs

   As shown in **Fig. 6d-f**, different concentrations of R6G were demonstrated because when concentration is quasi-single layer can be estimated. When the quasi-single layer is covered the MCuF surface, the molecular number is estimated by assuming the surface area of MCuFs. The picture of the right side shows high concentration (thick molecular layer), leading to loss of SERS enhancement, while the picture of the left side (single molecular layer) shows optimal concentration.

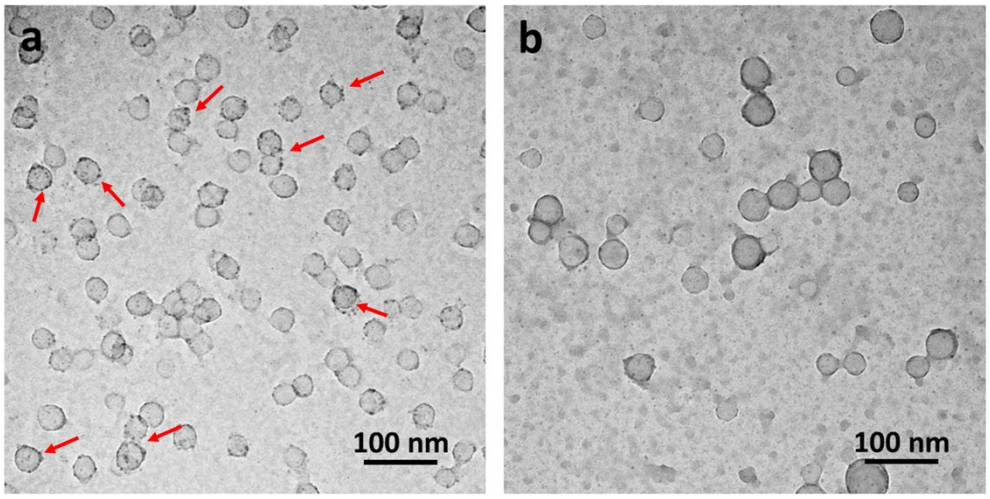

Fig. S1. The TEM images of PS_{63000}-*b*-PEO_{26000} spherical micelles (a) with Cu and (b) without Cu. The red arrows in **Fig. S1a** indicate Cu particles that stick around the micelles.

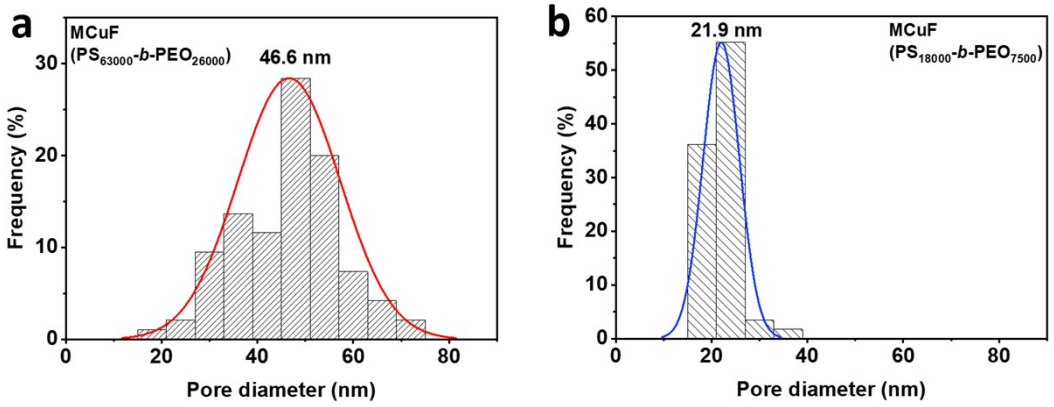

Fig. S2. Pore size distributions of MCuFs, **Fig. 2d** and **Fig. 4d**, using (a) PS_{63000}-*b*-PEO_{26000} and (b) PS_{18000}-*b*-PEO_{7500}.

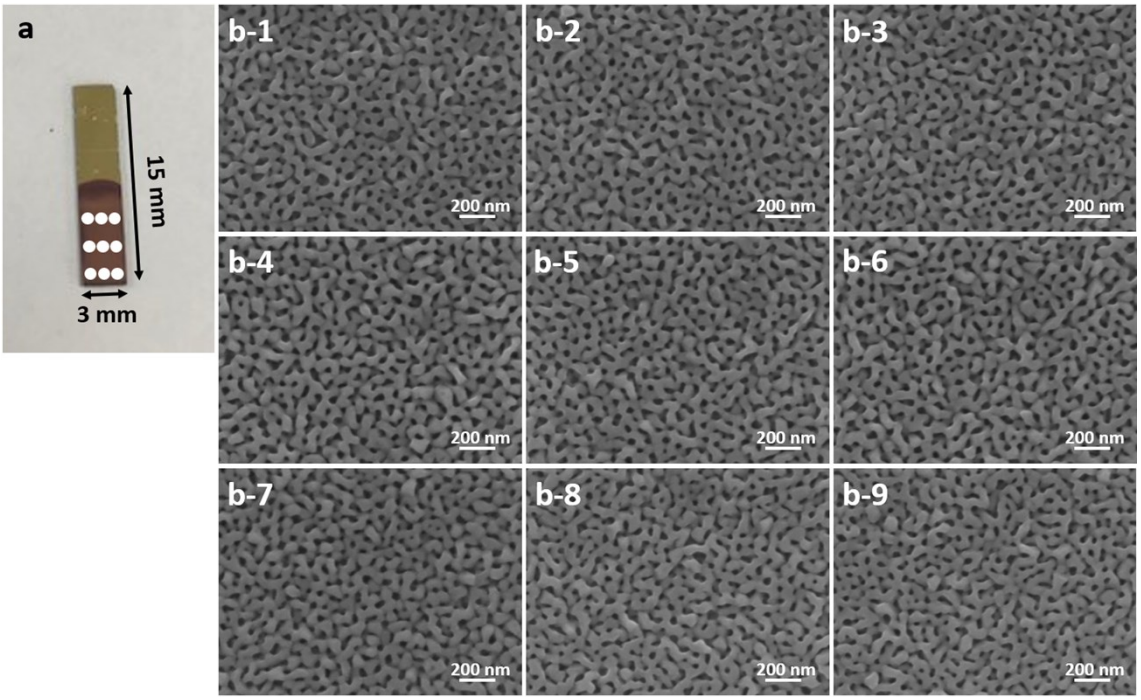

Fig. S3. (a) The photographic image and (b) SEM images of the MCuF using PS_{63000}-*b*-PEO_{26000} micelles on different positions. The electrodeposition condition is at -0.5 V for 600 s. The 9 positions (white dots) on (a) are corresponding to (b1-b9).

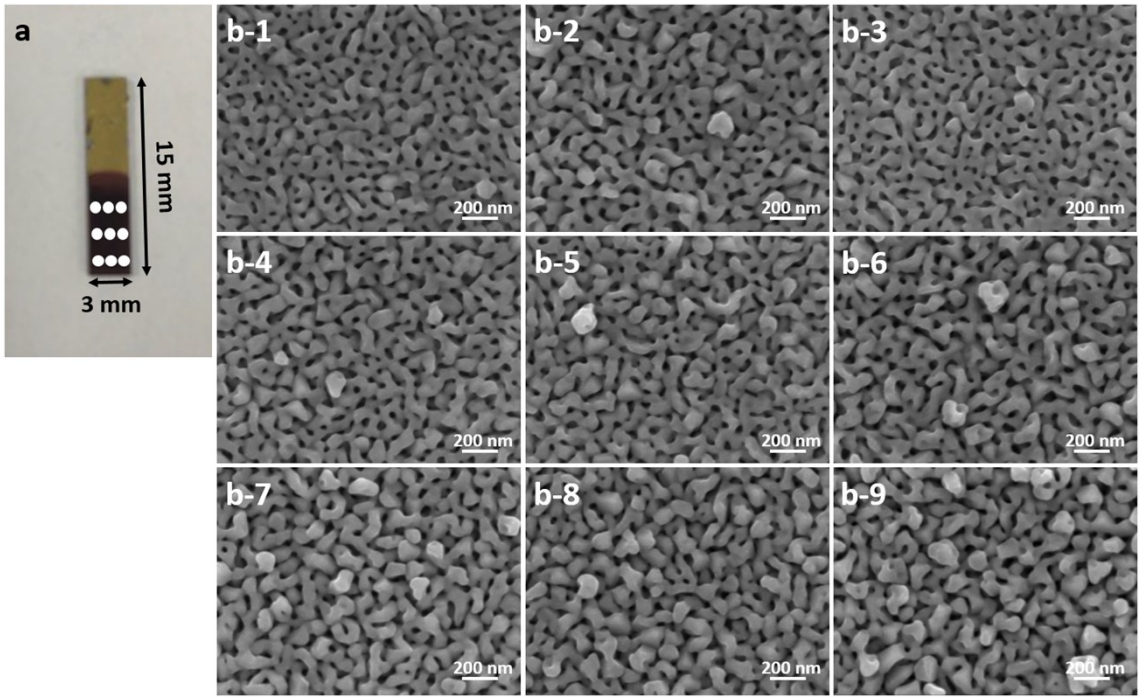

Fig. S4. (a) The photographic image and (b) SEM images of the MCuF using PS_{63000}-*b*-PEO_{26000} micelles on different positions. The electrodeposition condition is at -0.5 V for 1200 s. The 9 positions (white dots) on (a) are corresponding to (b1-b9).

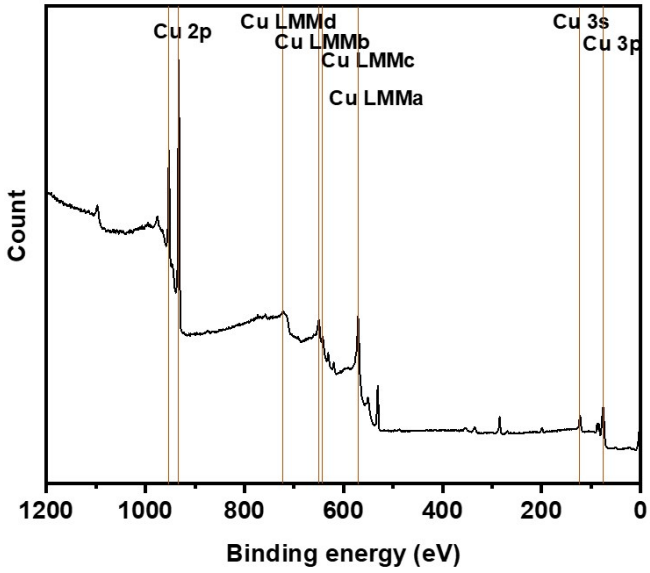

Fig. S5. The XPS survey of the MCuFs on the Au/Si substrate.

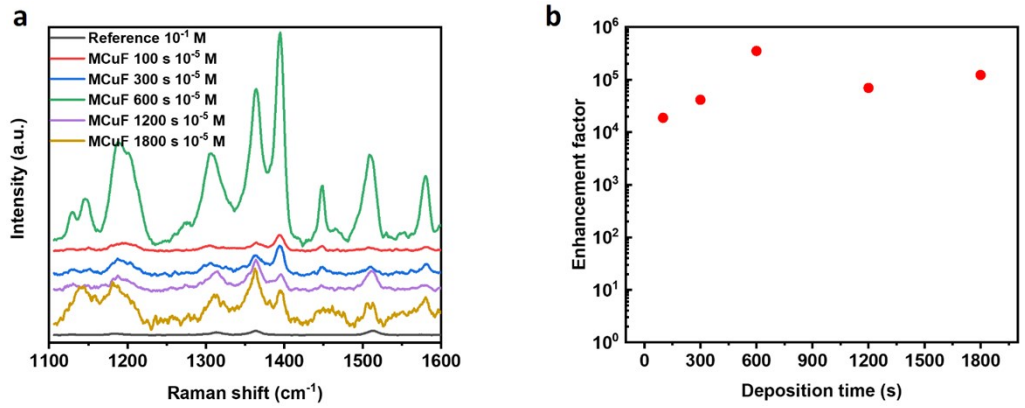

Fig. S6. (a) Raman spectra of R6G on a Si wafer (black line) and MCuFs using PS_{63000}-*b*-PEO_{26000} deposited at -0.5 V for different deposition times from 100 s to 1800 s. (b) Enhancement factors versus R6G concentrations calculated by 1361 cm^{-1} peak plots regarding the results of **Fig. S5a**.

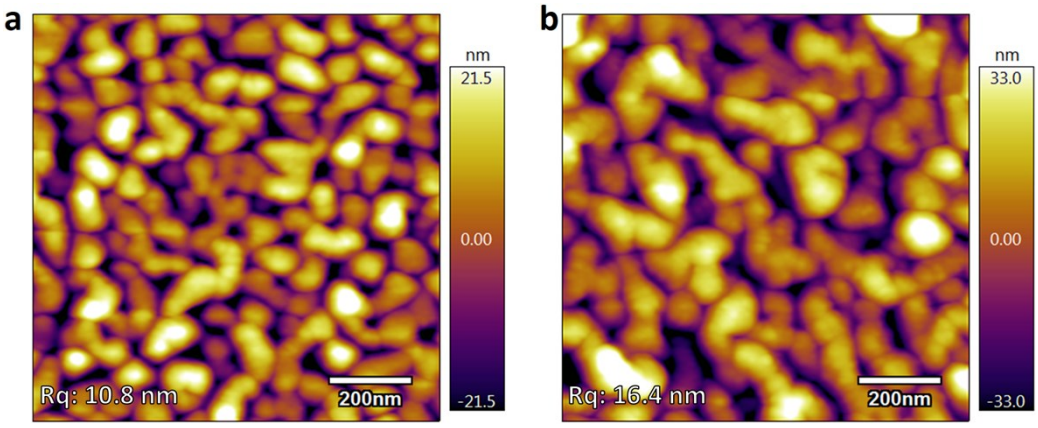

Fig. S7. AFM mappings of MCuFs deposited at -0.5 V for (a) 600 s (MCuF-1) and (b) 1200 s (MCuF-2). The Rqs for both substrates are (a) 10.8 nm and (b) 16.4 nm, respectively.

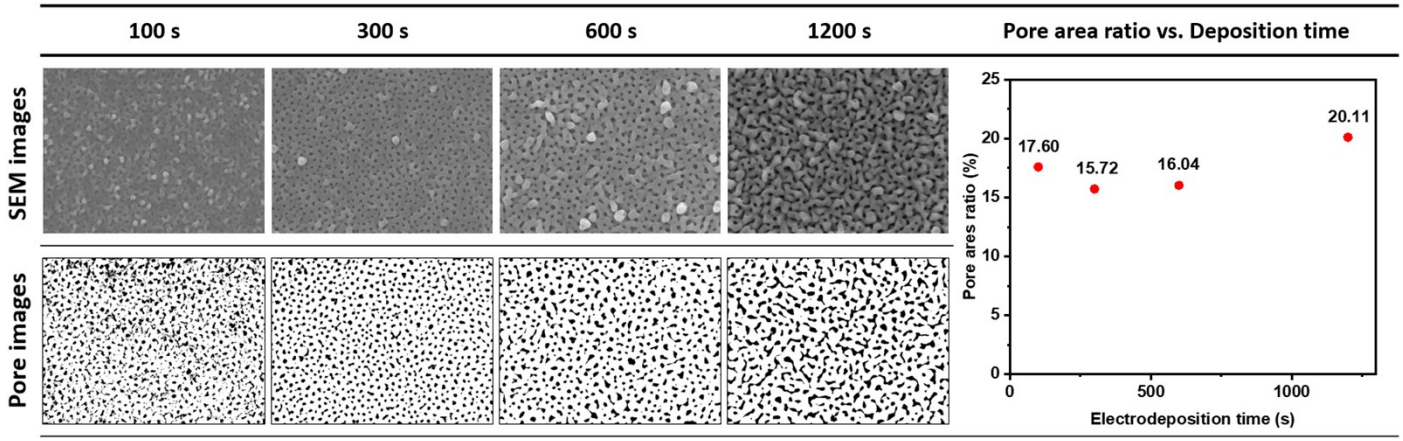

Fig. S8. The SEM and its monochromatic pore images of MCuFs with different deposition times. The plot on the right side shows the relation between the pore area ratio and the deposition times.

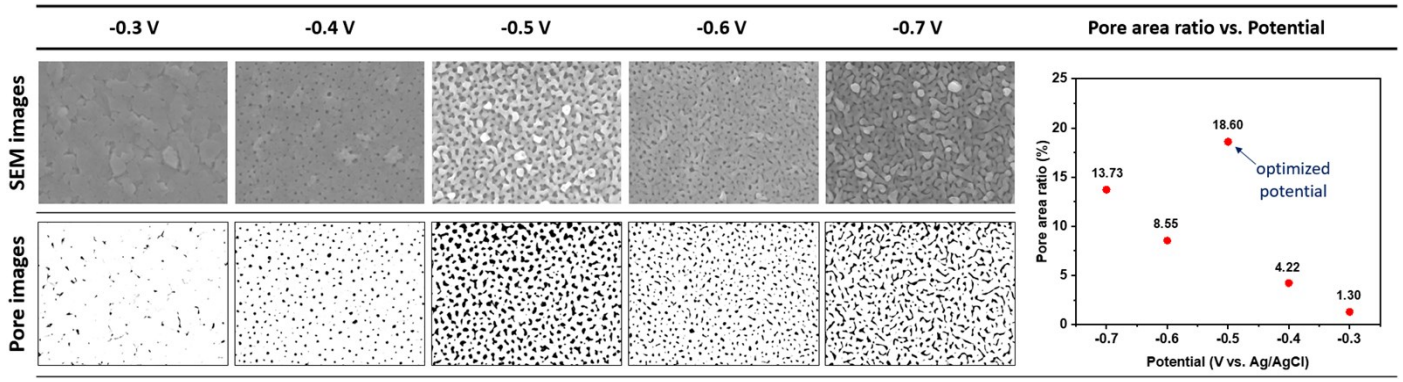

Fig. S9. The SEM and its monochromatic pore images of MCuFs with different deposition potentials. The plot on the right side shows the relation between the pore area ratio and the deposition potentials.

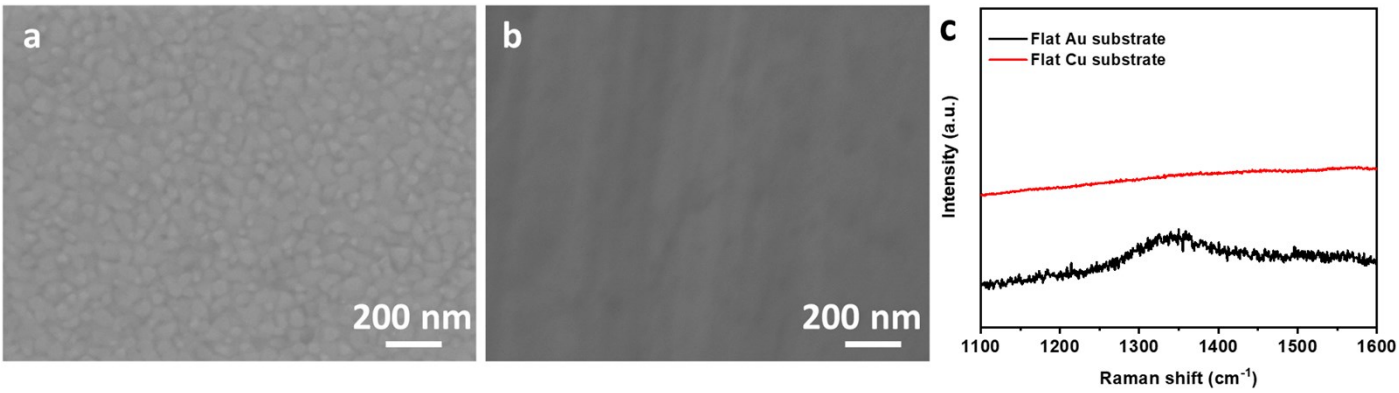

Fig. S10. SERS on flat metal films. The SEM image of (a) Au and (b) Cu films. (c) The SERS results of those two films with 10^{-5} M R6G.

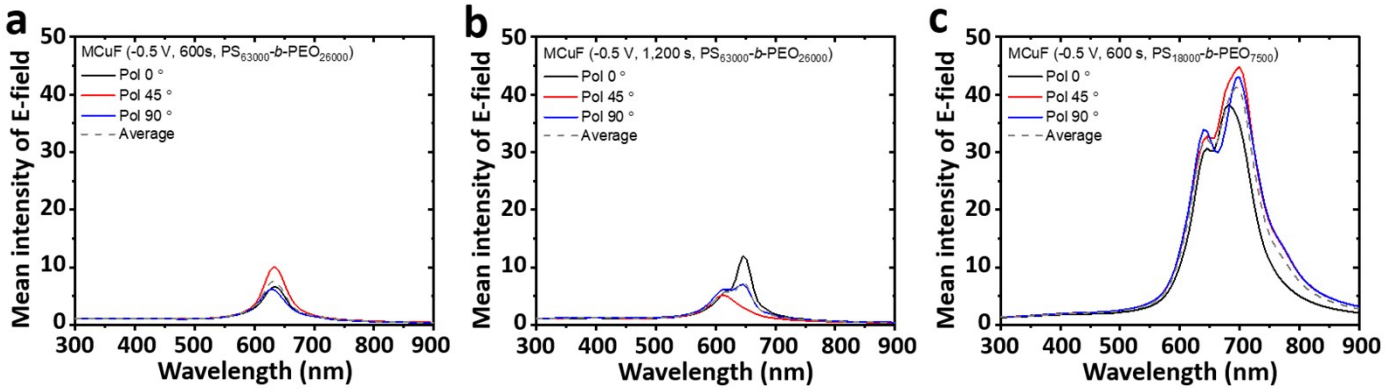

Fig. S11. The optical simulation of E-field spectra of MCuFs using PS_{63000}-*b*-PEO_{26000} (a) at -0.5 V for 600 s, (b) -0.5 V for 1200 s, and (c) using PS_{18000}-*b*-PEO_{7500} at -0.5 V for 600 s. Corresponding SEM images are in **Figs. 7a, 7b** and **7c**, respectively.

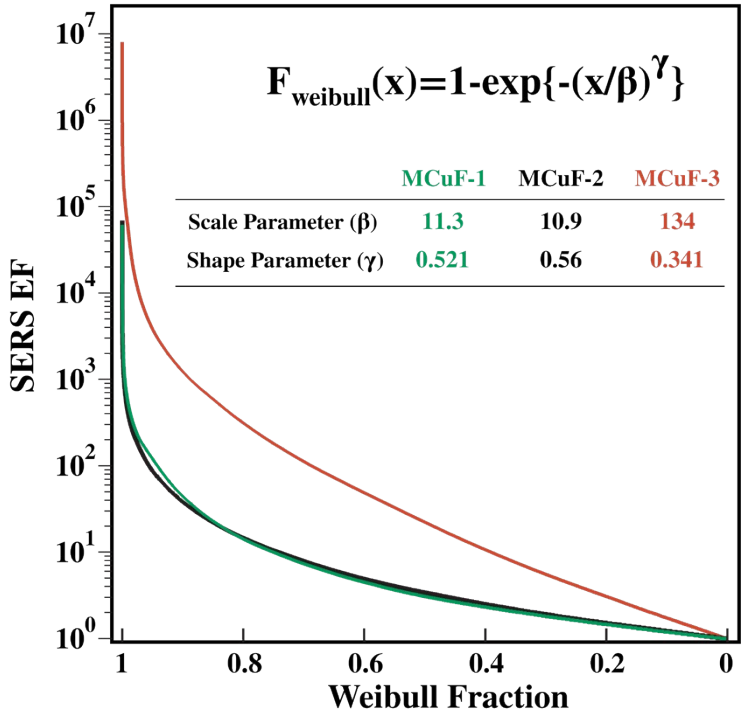

Fig. S12. A Weibull analysis was performed on the FDTD generated data in **Figures 7a-c**. Inset is the Weibull equation and a table showing the shape and scale parameters for each sample corresponding to MCuF-1, MCuF-2 and MCuF-3. A shape parameter (γ) less than 1 indicates the distribution of EFs has a long tail. MCuF-3 has a scale parameter (β) >10-times larger than the other samples, corresponding to a much larger average magnitude of EFs.

Table S1 The comparison with SERS results using MCuF plasmonic substrates.

Sample	Excitation (nm)	Potential	Time	Micelle (Mw of PS-b-PEO)	Enhancement Factor					LoD (M)
					10^{-2} M	10^{-3} M	10^{-4} M	10^{-5} M	10^{-6} M	
MCuF-1	785	-0.5 V	600	63000-26000	6.5×10^{2}	3.6×10^{3}	4.3×10^{4}	7.9×10^{4}	8.5×10^{4}	10^{-6}
MCuF-2	785	-0.5 V	1200	63000-26000	3.7×10^{3}	1.5×10^{4}	4.7×10^{4}	4.0×10^{4}	N/A	10^{-5}
MCuF-3	785	-0.5 V	600	18000-7500	2.5×10^{3}	1.4×10^{4}	7.8×10^{4}	1.0×10^{5}	3.8×10^{5}	10^{-6}

Table S2 The comparison with previous reports on SERS studies using Cu**.**

	Excitation (nm)	Analyte	Substrate size	Process step	EF_{max}	LoD (M)
Cu nanoparticle [S1]	514.5, 785	R6G 4-MBA	1 um	Multi	1×10^5	10^{-6}-10^{-7}
Cu Nanocrystal [S2] **(sword shape)**	785	4-MBA	Ununiform micrometer-scale	One	10^7	10^{-5}
Cu nanoparticle [S3]	633	R6G	Un	Multi	2.29×10^7	10^{-9}
Cu nanowire [S4]	N/A	R6G	50-100 nm	Multi	N/A	10^{-12}
Cu nanoparticle /Graphene [S5]	532	Copper phthalocyanine	45 nm	Multi	1.87×10^7	-
Nanoporous Cu film [S6]	514.5	R6G Crystal violet	Unlimited	Multi	1.85×10^5	10^{-5}
Triangular Cu nanoparticles [S7]	-	-	20-70 nm	Multi	-	-
Cu Nanoparticle [S8]	633	4-mercaptopyridine	40-50 nm	Multi	5.1×10^4	-
Roughened Cu foil [S9]	662	Nile blue *p*-nitrobenzoic acid	Unlimited	Multi	10^3-10^4 10^5-10^6	-
Mesoporous Cu film (This work)	785	R6G	Unlimited	One	3.8×10^5	10^{-6}

References

S1 C. Kong, S. Sun, X. Zhang, X. Song and Z. Yang, *CrystEngComm*, 2013, **15**, 6136-6139.

S2 X. Zhao, M. Deng, G. Rao, Y. Yan, C. Wu, Y. Jiao, A. Deng, C. Yan, J. Huang, S. Wu, W. Chen, T. Lei, P. Xu, W. He and J. Xiong, *Small*, 2018, **14**, 1802477.

S3 Q. Shao, R. Que, M. Shao, L. Cheng and S. T. Lee, *Adv. Funct. Mater.*, 2012, **22**, 2067-2070

S4 D. Xu, Z. Dong and J. L. Sun, *Mater. Lett.*, 2013, **92**, 143-146

S5 X. Li, X. Ren, Y. Zhang, W. C. H. Choy and B. Wei, *Nanoscale*, 2015, **7**, 11291-11299.

S6 L. Y. Chen, J. S. Yu, T. Fujita and M. W. Chen, *Adv. Funct. Mater.*, 2009, **19**, 1221-1226.

S7 G. H. Chan, J. Zhao, E. M. Hicks, G. C. Schatz and R. P. Van Duyne, *Nano Lett.*, 2007, **7**, 1947-1952.

S8 Y. Wang and T. Asefa, *Langmuir*, 2010, **26**, 7469-7474.

S9 S. K. Miller and A. Baiker, *J. Chem. Soc., Faraday Trans.*, 1984, **80**, 1305-1312.